

# Thermal photon statistics in spontaneous parametric downconversion

Fabio Paleari and Alessandra Andreoni

Dipartimento di Fisica e Matematica, Università degli Studi dell'Insubria and  
Istituto Nazionale per la Fisica della Materia, Unità di Como,  
Via Valleggio, 11 - 22100 Como, Italy  
[Fabio.Paleari@uninsubria.it](mailto:Fabio.Paleari@uninsubria.it) [Alessandra.Andreoni@uninsubria.it](mailto:Alessandra.Andreoni@uninsubria.it)

Guido Zambra

Istituto Nazionale per la Fisica della Materia, Unità di Como, Via Valleggio, 11 – 22100 Como, Italy, and  
Dipartimento di Fisica, Università degli Studi di Milano, Via Celoria, 16 – 20133 Milan, Italy  
[Guido.Zambra@unimi.it](mailto:Guido.Zambra@unimi.it)

Maria Bondani

Istituto Nazionale per la Fisica della Materia, Unità di Como, Via Valleggio, 11 – 22100 Como, Italy  
[Maria.Bondani@uninsubria.it](mailto:Maria.Bondani@uninsubria.it)

**Abstract:** We investigate photon statistics in the signal beam generated by frequency nondegenerate parametric downconversion both with and without a seed field along the idler direction. The experiments are performed on the signal generated in  $\beta$ -barium borate by a traveling-wave pump pulse that is the frequency-tripled output of an amplified Nd:YLF picosecond laser. The high powers obtained allow us to measure the number of photons with a simple detection technique. When both signal and idler fields are initially in their vacuum states, the generated fields are mixtures of equally occupied modes with thermal photon-number statistics.

©2004 Optical Society of America

**OCIS codes:** (270.6570) Squeezed states, (270.5290) Photon statistics, (190.4970) Parametric oscillators and amplifiers.

---

## References and links

1. Z. Y. Ou and L. Mandel, "Violation of Bell's inequality and classical probability in a two-photon correlation experiment," *Phys. Rev. Lett.* **61**, 50-53 (1988), [http://prola.aps.org/pdf/PRL/v61/i1/p50\\_1](http://prola.aps.org/pdf/PRL/v61/i1/p50_1).
2. Y. H. Shih and C. O. Alley, "New type of Einstein-Podolsky-Rosen-Bohm experiment using pairs of light quanta produced by optical parametric down conversion," *Phys. Rev. Lett.* **61**, 2921-2924 (1988), [http://prola.aps.org/pdf/PRL/v61/i26/p2921\\_1](http://prola.aps.org/pdf/PRL/v61/i26/p2921_1).
3. P. G. Kwiat, K. Mattle, H. Weinfurter, A. Zeilinger, A. V. Sergienko, and Y. Shih, "New high-intensity source of polarization-entangled photon pairs," *Phys. Rev. Lett.* **75**, 4337-4341 (1995), [http://prola.aps.org/pdf/PRL/v75/i24/p4337\\_1](http://prola.aps.org/pdf/PRL/v75/i24/p4337_1).
4. D. Boumeester, J. W. Pan, K. Mattle, M. Eibl, H. Weinfurter, and A. Zeilinger, "Experimental quantum teleportation," *Nature (London)* **390**, 575-579 (1997), [http://www.nature.com/cgi-taf/DynaPage.taf?file=/nature/journal/v390/n6660/full/390575a0\\_fs.html&content\\_filetype=PDF](http://www.nature.com/cgi-taf/DynaPage.taf?file=/nature/journal/v390/n6660/full/390575a0_fs.html&content_filetype=PDF).
5. D. Boschi, S. Branca, F. De Martini, L. Hardy, and S. Popescu, "Experimental realization of teleporting an unknown pure quantum state via dual classical and Einstein-Podolsky-Rosen channels," *Phys. Rev. Lett.* **80**, 1121-1125 (1998), [http://prola.aps.org/pdf/PRL/v80/i6/p1121\\_1](http://prola.aps.org/pdf/PRL/v80/i6/p1121_1).
6. A. Furusawa, J. L. Sørensen, S. L. Braunstein, C. A. Fuchs, H. J. Kimble, and E. S. Polzik, "Unconditional quantum teleportation," *Science* **282**, 706-709 (1998), <http://www.sciencemag.org/cgi/content/abstract/282/5389/706>.
7. B. R. Mollow and R. J. Glauber, "Quantum theory of parametric amplification. II," *Phys. Rev.* **160**, 1097-1108 (1967), [http://prola.aps.org/pdf/PR/v160/i5/p1097\\_1](http://prola.aps.org/pdf/PR/v160/i5/p1097_1).
8. D. T. Smithey, M. Beck, M. G. Raymer, and A. Faridani, "Measurement of the Wigner distribution of the density matrix of a light mode using optical homodyne tomography: application to squeezed states and the vacuum," *Phys. Rev. Lett.* **70**, 1244-1247 (1993), [http://prola.aps.org/abstract/PRL/v70/i9/p1244\\_1](http://prola.aps.org/abstract/PRL/v70/i9/p1244_1).
9. M. S. Kim, J.Y. Lee, D. Ahn, and P. L. Knight, "Entanglement induced by a single-mode heat environment," *Phys. Rev. A* **65**, 040101(R) (2002), <http://link.aps.org/abstract/PRA/v65/e040101>.
10. R. Loudon, *The Quantum Theory of Light*, 3<sup>rd</sup> ed. (Oxford U. Press, Oxford, 2000).

11. A. Beržanskis, W. Chinaglia, L. A. Lugiato, K.-K. Feller, and P. Di Trapani, "Spatial structures in optical parametric amplification," *Phys. Rev. A* **60**, 1626-1635 (1999), [http://prola.aps.org/pdf/PRA/v60/i2/p1626\\_1](http://prola.aps.org/pdf/PRA/v60/i2/p1626_1).
12. L. Mandel and E. Wolf, *Optical Coherence and Quantum Optics* (Cambridge U. Press, Cambridge, 1995), Chap. 14.
13. G. Zambra, M. Bondani, A. S. Spinelli, F. Paleari, and A. Andreoni, "Counting photoelectrons in the response of a photomultiplier tube to single picosecond light pulses," *Rev. Sci. Instrum.* (to be published).
14. D. Achilles, C. Silberhorn, C. Śliwa, K. Banaszek, and I. A. Walmsley, "Fiber-assisted detection with photon number resolution," *Opt. Lett.* **28**, 2387-2389 (2003), <http://ol.osa.org/abstract.cfm?id=78027>.
15. M. J. Fitch, B. C. Jacobs, T. B. Pittman, and J. D. Franson, "Photon-number resolution using time-multiplexed single-photon detectors," *Phys. Rev. A* **68**, 043814 (2003), <http://link.aps.org/abstract/PRA/v68/e043814>.
16. E. Brambilla, A. Gatti, M. Bache, and L. A. Lugiato, "Simultaneous near-field and far-field spatial quantum correlations in the high-gain regime of parametric down-conversion," *Phys. Rev. A* **69**, 023802 (2004), <http://link.aps.org/abstract/PRA/v69/e023802>.
17. M. Vasilyev, S.-K. Choi, P. Kumar, and G. M. D'Ariano, "Investigation of the photon statistics of parametric fluorescence in a traveling-wave parametric amplifier by means of self-homodyne tomography," *Opt. Lett.* **23**, 1393-1395 (1998), <http://ol.osa.org/abstract.cfm?id=36936>.
18. P. L. Voss, R.-Y. Tang, and P. Kumar, "Measurement of the photon statistics and the noise figure of a fiber-optic parametric amplifier," *Opt. Lett.* **28**, 549-551 (2003), <http://ol.osa.org/abstract.cfm?id=71651>.
19. Y. Zhang, K. Kasai, and M. Watanabe, "Investigation of the photon-number statistics of twin beams by direct detection," *Opt. Lett.* **27**, 1244-1246 (2002), <http://ol.osa.org/abstract.cfm?id=69376>.
20. M. M. Munroe, D. Boggavarapu, M. E. Anderson, and M. G. Raymer, "Photon-number statistics from the phase-averaged quadrature-field distribution: theory and ultrafast measurement," *Phys. Rev A* **52**, R924-R927 (1995), <http://link.aps.org/abstract/PRA/v52/pR924>.

## 1. Introduction

The main interest in the two-mode (signal and idler) squeezed vacuum states produced by nondegenerate spontaneous parametric downconversion lies in the relations between their interbeam and intrabeam properties. The interbeam photon correlation properties provide the characteristics needed for a wide range of experiments that are relevant to fundamental optics and quantum mechanics as well as to more-practical applications in quantum information and quantum computation [1–6]. Intrabeam properties are useful not only as diagnostic tools for determining the quantum nature of the field [7,8] but also as mediators of entanglement [9]. Here we focus on intrabeam properties, in particular, on the fact that the two beams individually display all the properties of chaotic (i.e., thermal) light [7,10].

It is easy to demonstrate theoretically that the photon-number statistics in each part of a twin beam are thermal for the single signal and idler modes obtained in conditions of phase matching when the pump is a monochromatic plane wave (and is nondepleted). However, in the concrete situation of an experiment, spontaneous parametric downconversion operates over a broad bandwidth of frequencies; i.e., the fields that are generated are characterized by finite coherence times. The fact that, for each of the twin beams, modes of different temporal frequencies propagate at the same angle to the pump wave vector [11] can be either relevant to the intrabeam photon number statistics or not. As long as the modes can be considered stationary fields, that is, over time intervals much shorter than the coherence time, the photon number statistics remain those of a single mode (with the expected mean photon number,  $\langle n \rangle$ ) [12], in our case

$$P(n) = \frac{1}{\langle n \rangle} \exp\left(-\frac{n}{\langle n \rangle}\right). \quad (1)$$

If the photon numbers are counted over intervals longer, say, by a factor  $m$ , than the coherence time, the photon-number statistic distribution becomes a multimode distribution that corresponds to  $n$  photons distributed over  $m$  equally occupied thermal modes [12], that is,

$$P_m(n) = \frac{\exp\left(-\frac{n}{N/m}\right)}{(N/m)^m} \times \frac{n^{m-1}}{(m-1)!}, \quad (2)$$

in which  $N$  denotes the mean photon number.

Our aim in this research is to prove Eq. (2) by analyzing the photon-number statistics in the signal beam generated by a high-gain traveling-wave optical parametric amplifier. Inasmuch as we achieve intense spontaneous parametric generation, the photon-number probability distributions are measured as pulse-height spectra of the current output of a Si-P-I-N photodiode detecting the signal pulses.

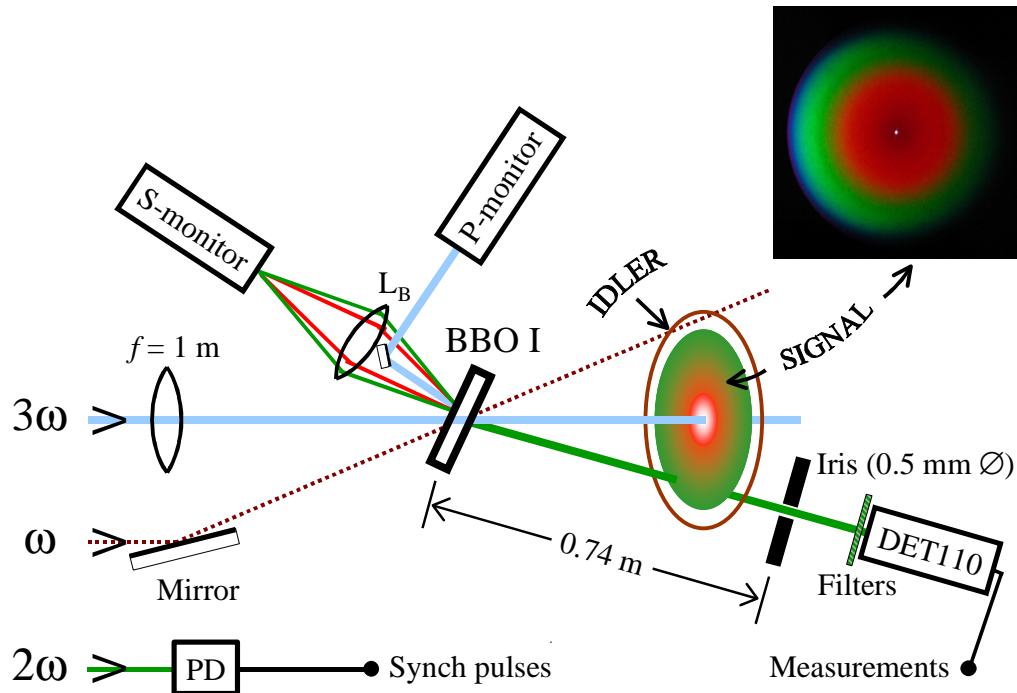


Fig. 1. Layout of the experimental setup. The outputs (fundamental,  $\omega$ ; second-harmonic,  $2\omega$ ; third-harmonic,  $3\omega$ ) of the picosecond amplified Nd:YLF laser serve as: pump ( $3\omega$ ); an idler seed when necessary ( $\omega$ ); synchronous trigger ( $2\omega$ ) for the measuring apparatus via the photodiode, PD. BBO I is a nonlinear crystal with type I interaction. Lens  $L_B$  focuses the signal cone reflected by BBO I onto the S monitor (photodiode monitoring the signal-cone energy). The blank at the  $L_B$  center is actually a small mirror reflecting the pump reflected by BBO I onto the P monitor (photodiode monitoring the pump-pulse energy). The animation shows photographs of the signal cones striking the wall of the laboratory (see text for details).

## 2. Experiments

As the pump source we use a frequency-tripled continuous-wave mode-locked Nd:YLF laser that was regeneratively amplified at a repetition rate of as much as 1 kHz (High Q Laser

Production, Hohenems, Austria). The laser was operated at a 500-Hz repetition rate throughout the research reported here. The experimental setup is sketched in Fig. 1. The  $3\omega$  beam (wavelength, 349 nm) is focused by a lens of 1-m focal length to give a spot of  $575 \pm 5 \mu\text{m}$  full width at half-maximum (FWHM) diameter, corresponding to a spot area of  $2.6 \times 10^{-3} \text{ cm}^2$  at the position of the nonlinear crystal. This is an uncoated  $\beta\text{-BaB}_2\text{O}_4$  crystal (Fujian Castech Crystals, Fuzhou, China) cut for type I interaction (cut angle, 22.8 deg) with a 10 mm  $\times$  10 mm cross section and 3-mm thickness (BBO I). With such a crystal, pump-pulse energies of tens of microjoules (pulse duration at  $\omega$ ,  $\sim 7.7$  ps FWHM for a Gaussian time profile) are sufficient to produce intense spontaneous parametric generation in broadly tunable cones. The animation in Fig. 1 shows photographs of the cones on the wall of the laboratory taken with a digital camera (400 ISO,  $f/2.9$ , 0.5 s) while the tuning angle was changed between successive exposures. The size of the photographed wall area was  $\sim 1.6 \text{ m} \times \sim 1.2 \text{ m}$ .

Here we describe experiments in which the  $3\omega$  beam was sent to the crystal at an (internal) angle of 33 deg to the optic axis (tuning angle). In one experiment we compared the statistics of the photons at  $2\omega$  in the signal cone starting from the vacuum state (spontaneous downconversion) to that obtained when a seed field at  $\omega$  was sent in the proper direction along the idler cone, a case in which notably negligible nonclassic effects were introduced in intrabeam properties by amplification [10]. In both cases the light to be measured was selected within a coherence area by an iris of 0.5-mm diameter that was located at a 74-cm distance from the crystal and centered with the seeded signal field at frequency  $2\omega$ . For brevity, in what follows, we call the signal light selected by the iris the signal at  $2\omega$  (see the green beam to the right of the artist's view of the broadband signal cone in Fig. 1). Because the photon fluxes were high in the absence of a seed also, detectors to resolve individual photons were not necessary [13], and arrays of time-multiplexed single-photon detectors were inapplicable [14,15]. A simple Si-P-I-N photodiode was more than sufficient to generate, on the average of the many realizations of the signal at  $2\omega$  that were necessary to collect significant statistical distributions, large-current pulses, of which we measured pulse-height spectra. The detector that we adopted was a DET110 photodiode (Thorlabs, Newton, N. J.) with  $\sim 20$ -ns FWHM response and a 3.6 mm  $\times$  3.6 mm sensitive area. A color filter with a transmittance of  $\sim 90\%$  in the visible was mounted in front of the DET110 photodiode to cut the stray pump light; the overall detection efficiency at 523.5 nm (signal at  $2\omega$ ) was  $\eta \cong 53\%$ . The photodiode current output was integrated over a synchronous gate of suitable time duration (50 ns) by a boxcar averager that was operated, as a gated integrator, in external trigger modality (see the photodiode, PD, in Fig. 1). The boxcar output was digitized by a 13-bit converter, and the counts were stored in a PC-based multichannel analyzer. We used either a 4121B averager (Perkin-Elmer, Oak Ridge, Tenn.) with full scale set at 20 mV or an SR250 instrument (Stanford Research Systems, Palo Alto, Calif.) with 50-mV full scale; the only difference between the two instruments is that one channel corresponds to a charge value,  $\Delta q$ , of 34,393 electrons in the former case and of 78,125 electrons in the latter. Another photodiode (PD in Fig. 1, with a pulse response of  $\sim 1$  ns) that detects the Nd:YLF second-harmonic pulse, also available as a (secondary) output of the laser system, provided the triggering signal to the boxcar averager. One obtains detection probabilities simply by normalizing the experimental pulse-height distributions to their integral values.

Ideally, each realization of the signal field at  $2\omega$  (and each count of the detected photons) should be acquired with a pump pulse of the same intensity profile in both time and space. For instance, each shot of the pump laser should be tested with a streak camera and with a beam analyzer, and afterward selection of the data should be made according to the time and space profiles detected by the two monitoring systems. As an alternative to this rather impractical experimental approach, we utilized similar electronics to acquire both the pump-pulse energy and the energy of the whole signal cone (whole cone) in parallel to each acquisition of the signal at  $2\omega$ . A fraction of the pump pulse before it entered BBO I was detected by a Thorlab DET210 photodiode (see the  $P$  monitor in Fig. 1), whereas the whole cone that was

backreflected by the BBO I output face was collected by a spherical lens,  $L_B$ , with a blank in the center to stop the reflected pump, and focused onto another DET110 detector ( $S$  monitor). The realizations of the signal at  $2\omega$  that we used to collect the data presented below were characterized by energies of the whole cone fluctuating by less than  $\sim 2.6\%$  (root-mean-square value) of the mean energy. The corresponding spread of the pump-pulse energy was below the resolution of our pulse-height spectral measurements. We believe that these two observations are good indications that the instantaneous intensity of the pump pulse at the crystal entrance is reproducible from shot to shot.

The experimental distributions of the probability of detecting photons in the signal at  $2\omega$  that are plotted in Fig. 2 (circles) refer to spontaneous downconversion in which the pump-pulse energy was  $\sim 360 \mu\text{J}$ . The various distributions in Fig. 2 were obtained

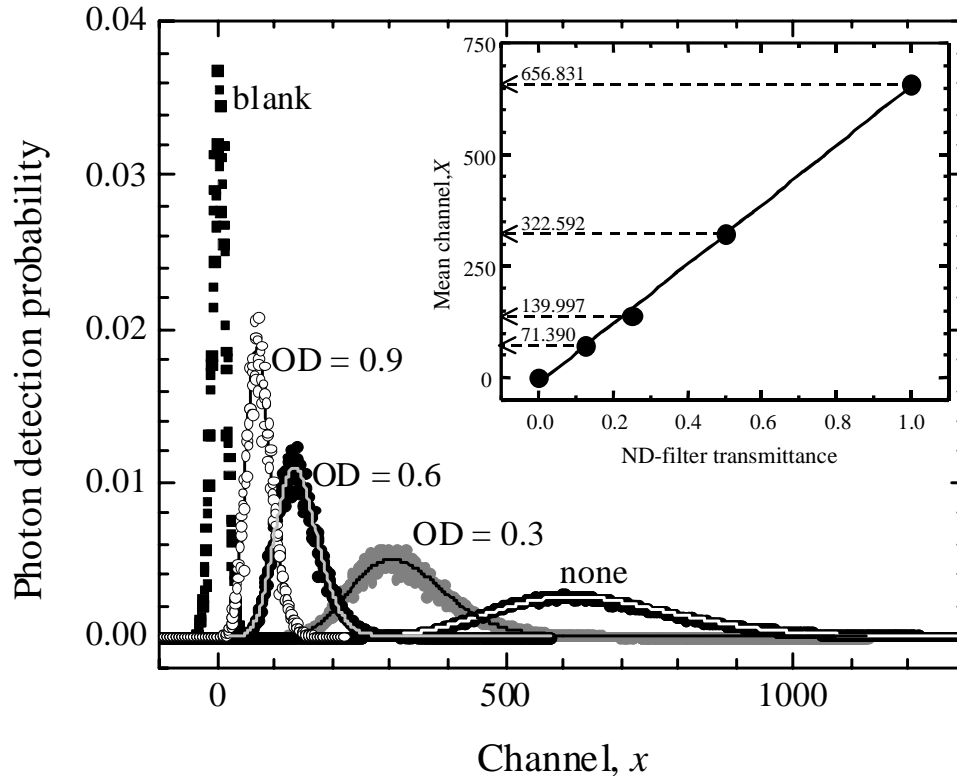


Fig. 2. Photon detection probability distributions as a function of channel number  $x$  for different ND filters on the signal at  $2\omega$  [optical-density (OD) values of the ND filters are indicated]. Experimental data, solid curves; numerical fits, *vide infra*. The inset shows the mean channel number,  $X$ , of the experimental distributions as a function of ND-filter transmittance, i.e.,  $10^{-\text{OD}}$ ; straight line, least-squares fit. For conversion to photon numbers:

$$n = (\Delta q / \eta) x, \text{ with } \Delta q = 78125 \text{ electrons/channel; see text.}$$

on insertion of different neutral-density (ND) filters of calibrated optical-density values in front of the detector. The squares in Fig. 2 mark the distribution that we measured when a blank was inserted. This distribution, which is actually symmetric about the peak channel over 4 orders of magnitude, was reproducible in both shape and position over time spans much longer than the time needed to acquire the entire set of measurements displayed in the figure. As it represents the system's response to zero detected photons, we assume that its mean channel is the zero channel,  $x = 0$ , in the horizontal scale in the figure. As shown in the inset, the mean channel values,  $X$ , of the experimental distributions for the various ND filters are rather accurately proportional to the filter transmittance values.

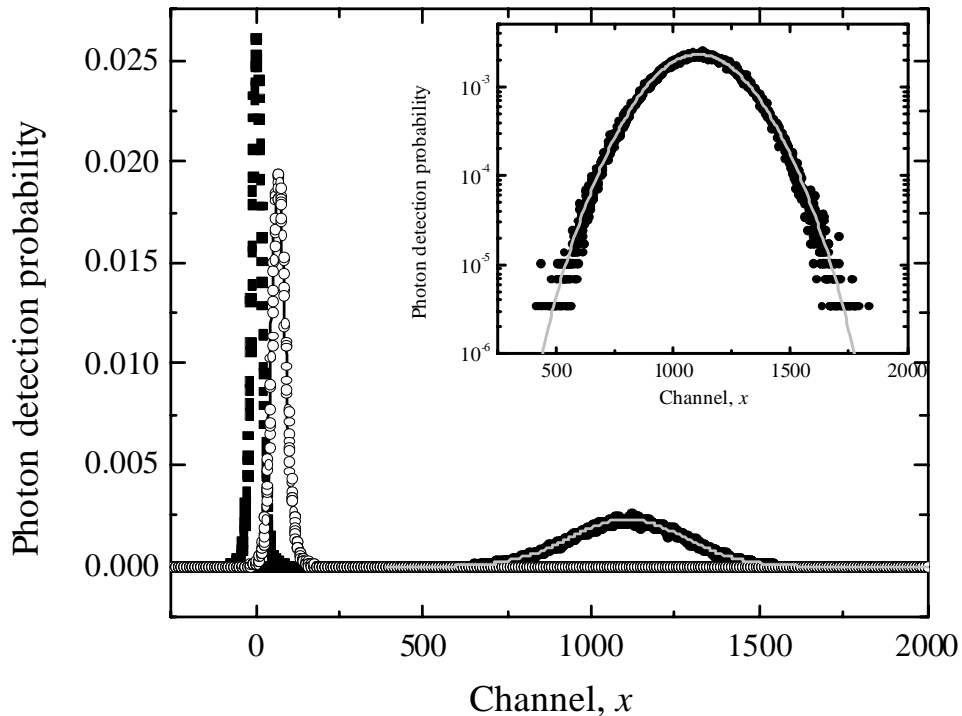


Fig. 3. Photon detection probability distributions in the signal at  $2\omega$  as a function of channel number  $x$  for spontaneous downconversion (open circles) and for downconversion with a seed idler pulse (filled circles). Square symbols, distribution for  $X = 0$ . Inset, logarithmic plot of the data for spontaneous downconversion and best-fitting Gaussian with a fixed mean value corresponding to the experimental  $X$  value. For conversion to photon numbers see Fig. 2 with  $\Delta q = 34393$  electrons/channel.

The experimental distributions of the probability of detecting photons in the signal at  $2\omega$  that are plotted in Fig. 3 (circles) refer to spontaneous downconversion (open circles) and to downconversion in which a seed pulse at  $\omega$  was injected along the idler cone (filled circles). The two distributions, which were measured for the same pump-pulse energy ( $\sim 260 \mu\text{J}$ ), gave  $X = 67.573$  and  $X = 1103.980$ , respectively.

### 3. Analysis of the results and discussion

First we recall that to interpret our data by using Eq. (2) amounts to making the assumption that the signal field to be measured is a mixture of  $m$  modes, each one populated by the same mean number of photons,  $N/m$ , where  $N$  is the mean number of photons in the pulses of the signal at  $2\omega$ . Moreover, we note that the direct results of our measurements are probability distributions of the number of detected photons rebinned into histograms with bin size  $\Delta q$  and that we detect the photons by a process with quantum efficiency  $\eta < 1$ . It can be demonstrated that both rebinning and convolution with the binomial distribution with parameter  $\eta$  applied to photon probability distribution  $P_m(n)$  in Eq. (2) give

$$P_m(x) = \frac{\exp\left(-\frac{x}{X/m}\right)}{(X/m)^m} \times \frac{x^{m-1}}{(m-1)!}, \quad (3)$$

in which  $x = (\eta/\Delta q)n$ . To fit the experimental distributions in Fig. 2, for each measurement with a given  $X$  value ( $X > 0$ ; see the values marked on the axis of the inset in Fig. 2) we calculated the convolution integrals with the system response (squares,  $X = 0$ , in Fig. 2) for a number of tentative  $m$  values. The solid curves in Fig. 2 are the convolution integrals that best fit the experimental distributions and correspond to  $m = 16$  in all cases except that for the highest intensity, in which the best fit was found for  $m = 17$ . Note that the mean numbers of photons in these measurements,  $N = (\Delta q/\eta)X$ , are  $10.523 \times 10^6$  to  $9.682 \times 10^7$ . Hence with our source we achieved single-mode populations of as many as  $\sim 5.7$  in  $10^6$  photons.

The experimental distributions of the probability of detecting photons in the signal at  $2\omega$  that are plotted in Fig. 3 (open circles, spontaneous downconversion; filled circles, with idler seed) correspond to  $N = 4.385 \times 10^6$  and  $N = 7.164 \times 10^7$  photons, respectively. The solid curves are best-fitting functions, which for the spontaneous process are calculated as above but for the seeded process are the best-fitting Gaussians of fixed mean value. The enlarged logarithmic plot in the inset of Fig. 3 shows the reliability of this fit over 3 orders of magnitude. This result agrees with the fact that in the presence of the idler seed the parametric amplifier works as a classic amplifier [10]. Note that in Fig. 2 we found multithermal-mode photon statistics even when the mean photon number was greater than that measured for the Gaussian distribution displayed in Fig. 3.

As anticipated in Section 1, the good agreement of the experimental results in the case of spontaneous downconversion with probability distribution  $P_m(n)$  in Eq. (2) suggests that we interpret the number of modes,  $m$ , as the ratio of the time over which we collect the photons to be counted,  $T$ , to the coherence time,  $\tau_s$ , of the signal at  $2\omega$  [12]. Inasmuch as we simply measure the number of photons,  $n$ , in the spontaneously downconverted signal in each pump pulse, it is correct to identify  $T$  with the pump-pulse duration [16]. Thus  $m$  should be interpreted as  $m = T_p/\tau_s = T_p\Delta\omega_s/(8\ln 2)$ , in which  $\Delta\omega_s$  denotes the FWHM bandwidth of

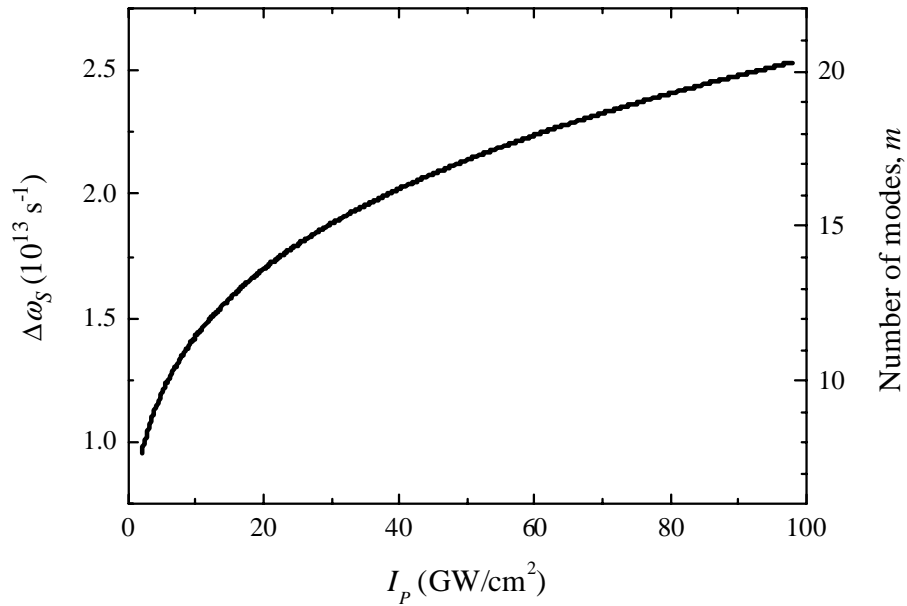


Fig. 4. Calculated FWHM bandwidth,  $\Delta\omega_s$  (left-hand scale), of the signal gain at  $2\omega$  for a nondepleted pump of intensity  $I_p$ . Right-hand scale, number of modes calculated as  $m = T_p \Delta\omega_s$ , where the pump-pulse duration,  $T_p$ , is assumed to be 4.45 ps (FWHM value).

the signal that is due to phase mismatch. Based on the FWHM duration of the amplified pulse at  $\omega$  generated by our Nd:YLF system, we assume that  $T_p \cong 4.45$  ps, i.e., the duration of the pulse at  $\omega$  divided by  $\sqrt{3}$  for the FWHM duration of the pump pulse at  $3\omega$ . The calculation of  $\Delta\omega_s$  for the experimental noncollinear interaction that occurs in our BBO I crystal as a function of the pump intensity  $I_p$ , which is assumed to be monochromatic and nondepleted, leads to the dependence depicted in Fig. 4. The right-hand vertical axis in the figure has been rescaled by the factor  $T_p / (8 \ln 2)$  to display the quantity that we should interpret as the number of modes,  $m$ . We can observe that the curve in Fig. 4 provides  $m$  values in the correct range. For example, the value  $m = 16$  that fits the majority of the distributions in Fig. 2 corresponds to  $I_p \cong 38$  GW/cm<sup>2</sup>, whereas in the experiment the peak pump intensity was  $\sim 29$  GW/cm<sup>2</sup> if it was calculated as pump peak power divided by spot area  $A$  (see above) but reached  $\sim 81$  GW/cm<sup>2</sup> at the center of the pump spot. Note that, in the calculation that leads to the curve in Fig. 4,  $I_p$  is the intensity of a continuous plane wave, a fact that is likely to represent a too-crude approximation in experiments that are performed with pulses of short duration and beams of finite cross section [17].



#### 4. Conclusions and perspectives

Research is in progress at our laboratory to refine the model underlying the calculation of the gain line shape in nondegenerate spontaneous parametric downconversion to include the actual temporal evolution of the pump pulse and its transverse spatial profile as well as to measure directly the coherence times of both pump and signal pulses by suitable interferometric techniques. However, we believe that the results shown in Fig. 4 already provide good support for the interpretation of the measured photon-number probability distributions by means of Eq. (2) and to the demonstration that in a broadband and intense parametric fluorescence signal the photons are equally distributed over a number of thermal modes that is determined by the ratio of measure time to coherence time.

We have also shown here that, when a parametric fluorescence signal is highly intense, demonstrating its thermal photon statistics becomes feasible with a rather simple detection technique. To date such a demonstration has been achieved for pulses containing tens of photons only by self-homodyne techniques [17,18] and, in part, by direct detection of the light and mixing the photocurrent with an electrical oscillation [19]. Obviously none of these works concerned fields with multithermal-mode photon statistics. Finally, we do not exclude that methods based on the measurement of phase-averaged quadrature-field distribution with ultrafast sampling [20] are suitable for characterizing the squeezed vacuum states generated by our system, in that we can obtain suitably short and powerful pulses for the local oscillator, but in the light of the experimental results described in this paper we consider the method described in [20] intrinsically overabundant for measuring photon-number statistics.

#### Acknowledgments

The authors are grateful to Matteo G. A. Paris (Università degli Studi, Milan) and to Alessandra Gatti [Istituto Nazionale per la Fisica della Materia (INFM), Como] for stimulating discussions and comments. The Ph.D. studies of Fabio Paleari are funded by the Istituto di Fisica del Plasma "Piero Caldirola," National Research Council, Milan. This research was partially supported by INFM through project "PRA CLON" and by the Italian Ministry for University Research through FIRB (Fondo per gli Investimenti della Ricerca di Base) project RBAU014CLC\_002.